Final Report: Seismic Analysis at Strategic Border Sites Trip 1: DTRA-OM5

Richard D. Miller, J. Tyler Schwenk, Julian Ivanov,
Shelby L. Peterie, J. Jordan Nolan, Brett Wedel,
Ryan Nelson, Brett Bennett, and Joe Anderson

Kansas Geological Survey
1930 Constant Avenue
Lawrence, KS 66047

Final Report to:

David Masters
U.S. Department of Homeland Security
Science & Technology Directorate
245 Murray Lane SW—MS0115
Washington, DC 20528-0115

John Lane, PhD
Branch of Geophysics
Office of Groundwater
U.S. Geological Survey
11 Sherman Place
Storrs-Mansfield, CT 06269

Open-File Report #2017-37 **November 5, 2013**

The Kansas Geological Survey makes no warranty or representation, either express or implied, with regard to the data, documentation, or interpretations or decisions based on the use of this data including the quality, performance, merchantability, or fitness for a particular purpose. Under no circumstances shall the Kansas Geological Survey be liable for damages of any kind, including direct, indirect, special, incidental, punitive, or consequential damages in connection with or arising out of the existence, furnishing, failure to furnish, or use of or inability to use any of the database or documentation whether as a result of contract, negligence, strict liability, or otherwise. This study was conducted in complete compliance with ASTM Guide D7128-05. All data, interpretations, and opinions expressed or implied in this report and associated study are reasonably accurate and in accordance with generally accepted scientific standards.

Final Report: Seismic Analysis at Strategic Border Sites
Trip 1: DTRA-OM5

Summary

The Kansas Geological Survey acquired 14 lines of active seismic data at 12 sites during two trips to the US-Mexico border. Data were processed using multi-channel analysis of surface waves (MASW), refraction tomography, and surface wave inversion to obtain 2-D profiles of shear-wave velocity (Vs), compressional-wave velocity (Vp), and seismic quality factor (Qs and Qp) for the near surface. This report contains final processing and results for the DTRA-OM5 site.

Data Acquisition

One line of seismic data (~287 m) was acquired on January 31, 2013, at DTRA-OM5 coincident with the USGS ERT profile (Figure 1). The system of sources and receivers, collectively, is the Active Seismic Imaging (ASI) system developed by and fabricated at the Kansas Geological Survey (Figure 2). Seismic sources were an accelerated weight drop for surface wave and long-offset compressional energy, sledge hammer and steel plate for near-offset compressional-wave energy, and sledge hammer and shear block for shear-wave energy. Seismic receivers were located in a towed 48-channel 3-component (3-C) land streamer with 24 stations separated by 1.2 m. Receivers were single 4.5 Hz vertical geophones and two 14 Hz horizontal (SV orientation) geophones (Figure 3). Seismographs were a Geometrics Geode distributed system. The survey was fixed spread with variable 0-57.3 m source offset (Figure 4) to obtain sufficient seismic sampling within the depth of interest. Individual receiver spreads overlapped by half of a spread.

Downhole data were acquired on August 13, 2013, approximately 575 m from center of seismic line, with a 3-C downhole Geostuff geophone (Figure 5). The shallowest receiver station was located at a depth of 1.5 m, and receiver station spacing was 0.75 m (Figure 6). A repeatable shear and compressional 9 kg hammer source, developed and fabricated at the Kansas Geological Survey, was located at 3 m from the borehole (Figure 7). A 2.7 kg sledge hammer and steel plate were located at 22.9 m from the borehole.

For both the surface and downhole seismic surveys, multiple shots were acquired and recorded separately for each unique shot/receiver configuration and stacked during processing to minimize ambient noise (Figure 8) and increase the signal-to-noise ratio.

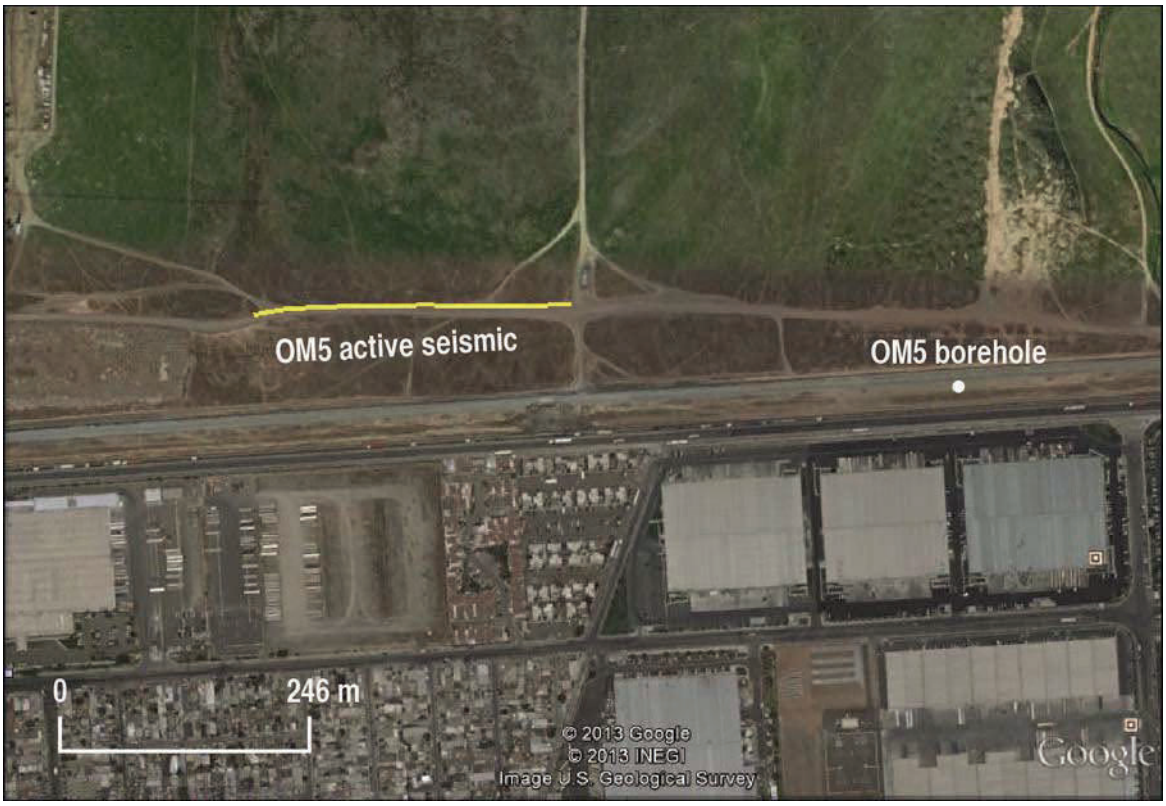

Figure 1: Aerial photo of DTRA-OM5 and the location of the active seismic line.

Figure 2: ASI and attached 48-channel 3-C land streamer utilized at OM5.

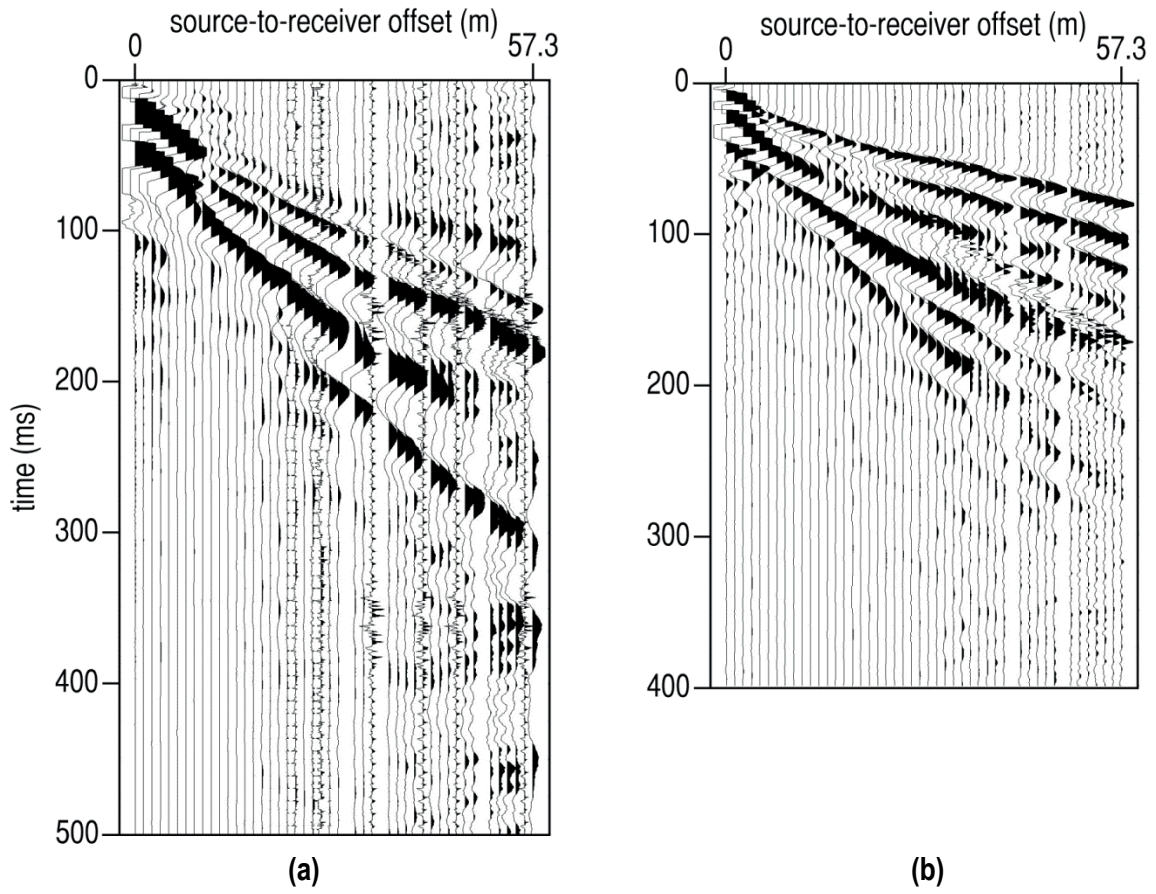

Figure 3: Representative off-end shot gathers at DTRA-OM5. (*a*) Sledge hammer and shear block source recorded with shear 14 Hz geophones, SV orientation. (*b*) Weight drop source recorded with 40 Hz vertical component geophones.

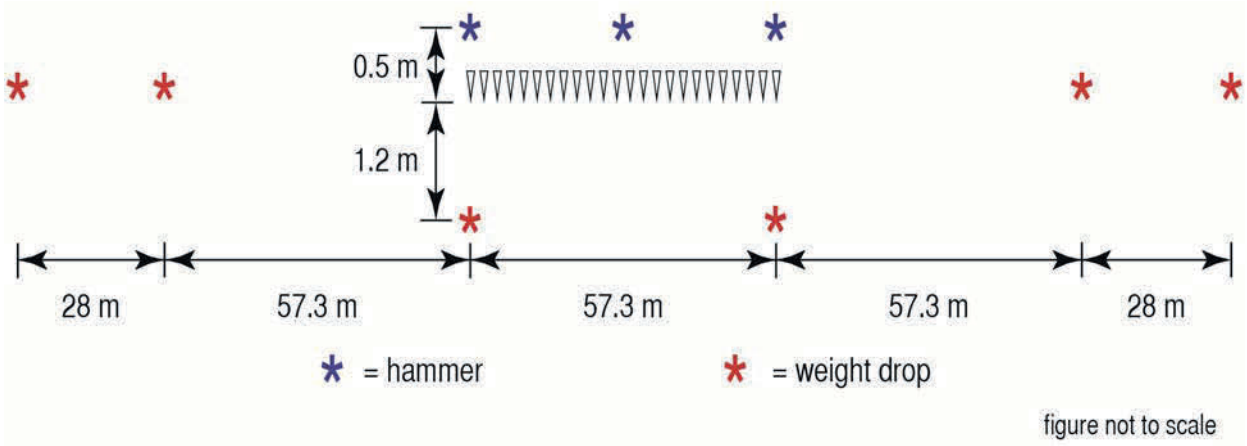

Figure 4: Diagram indicating all shot point locations relative to a single receiver spread.

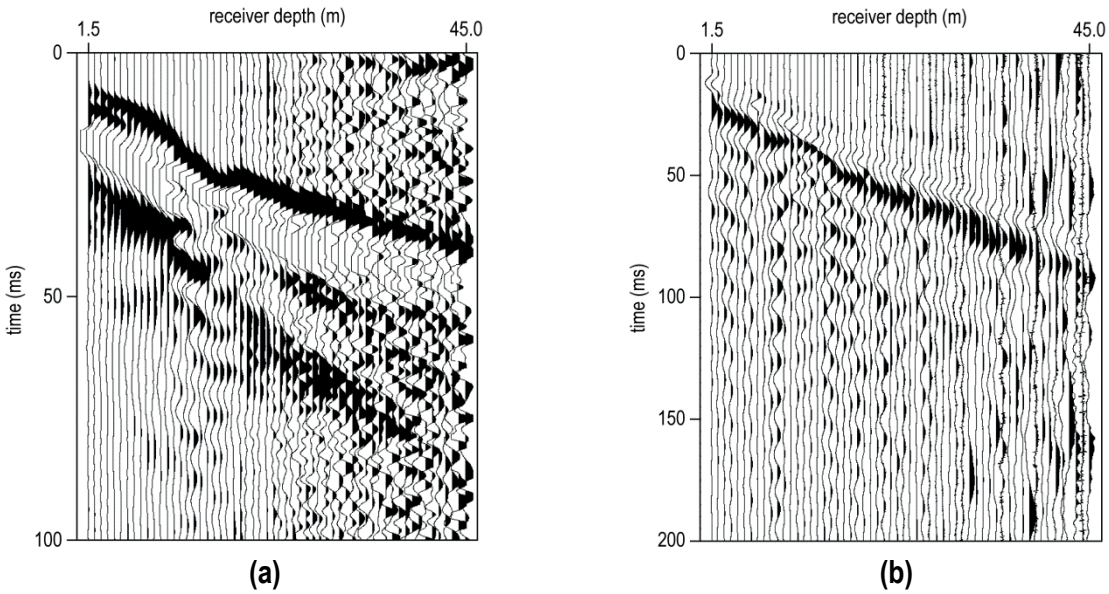

Figure 5: Representative downhole (*a*) vertical and (*b*) shear records at DTRA-OM5.

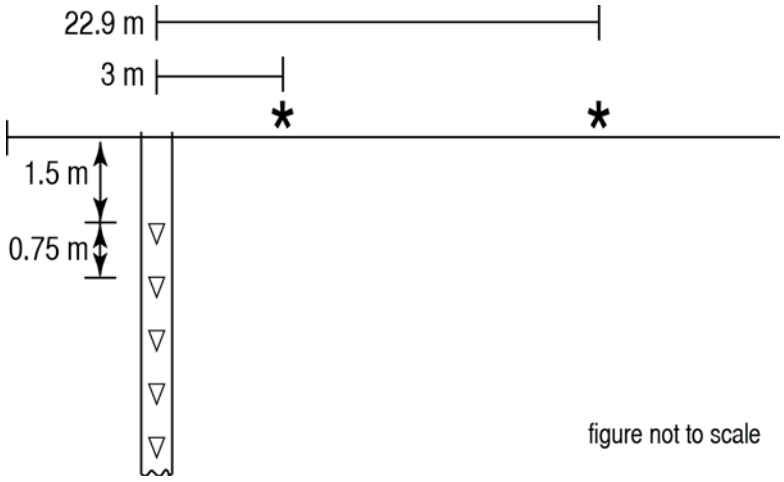

Figure 6: Downhole seismic field layout.

Figure 7: Downhole seismic acquisition utilized at DTRA-OM5.

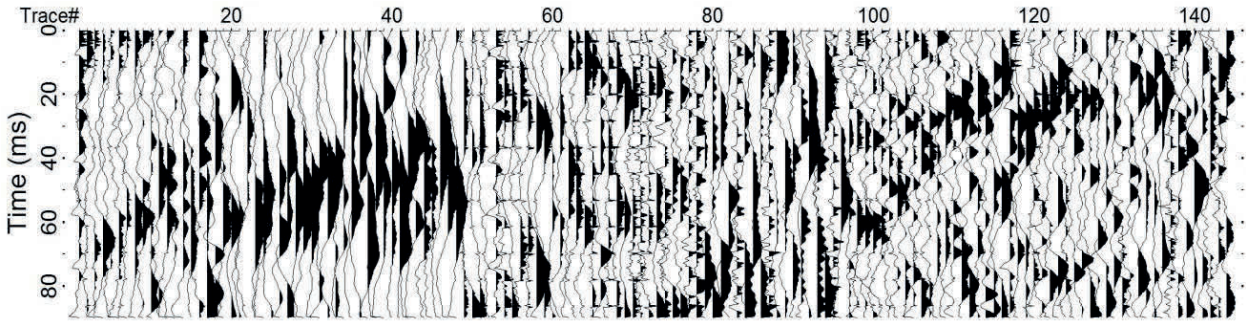

Figure 8: Representative ambient noise recorded at DTRA-OM5. Traces 1-48 represent the 4.5 Hz geophones, 49-96 represent the shear geophones, and 97-144 represent the 40 Hz geophones.

Data Processing

Multichannel-analysis of surface waves (MASW) was used to analyze dispersive Rayleigh-wave energy and estimate shear-wave velocity (Vs). Fundamental-mode energy was interpreted and inverted using a weighted, damped least-squares approach (Xia et al., 1999), resulting in a 2-D Vs profile. Average and interval downhole compressional-wave velocity (Vp) and Vs were calculated using the arrival time of the direct P-wave and S-wave, respectively, and pathlength from the seismic source to each receiver depth. Refraction tomography with 1.2 x 1.2 m cell size was used to estimate Vs and Vp. Joint-analysis of refractions and surface waves (JARS, Ivanov et al., 2010) was used to constrain the non-uniqueness inherently involved in refraction inversion, resulting in physically realistic 2-D Vs and Vp profiles. Shear- and compressional-wave seismic quality factors (Qs and Qp, respectively) were obtained using a surface wave inversion technique (Xia et al., 2010). Downhole shear records were numerically rotated to orient the recorded shear-wave traces in the vertical (SV) and horizontal (SH) polarization directions (Di Siena et al., 1984). The direct P-waves and S-waves were isolated on compressional and shear records, respectively, and the spectral ratio method was used to estimate Qp and Qs for each lithology identified in drilling notes (Tonn, 1991; Hasse and Stewart, 2004). The velocity and quality values calculated from downhole data were used to constrain inversion and improve accuracy of the results obtained using surface seismic methods.

Final Results

MASW

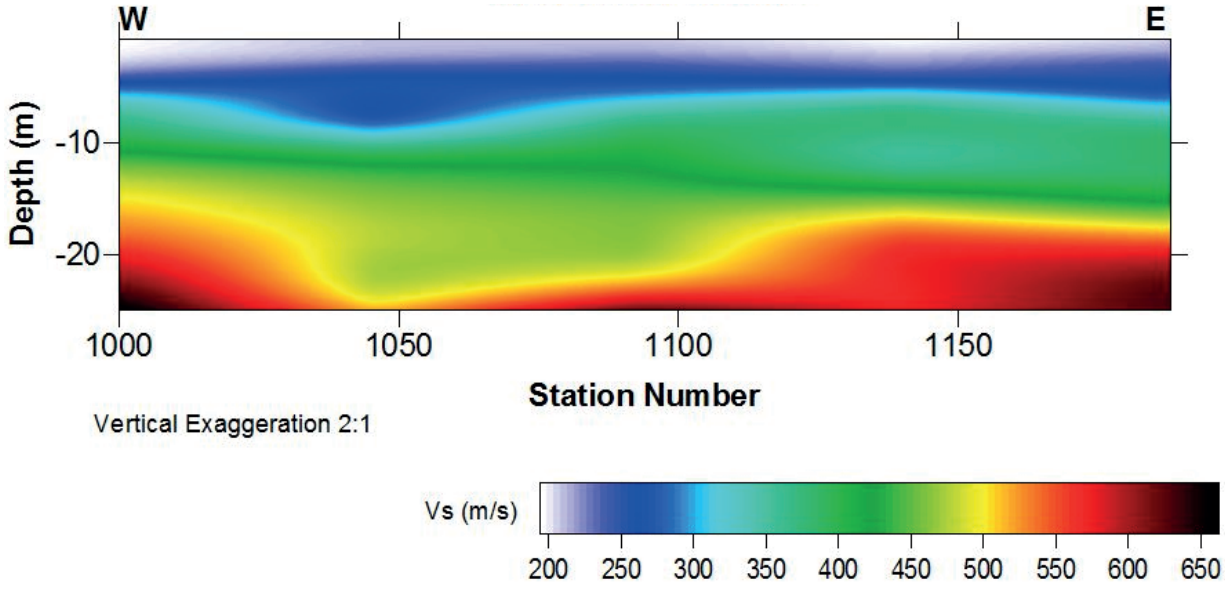

Figure 9: MASW Vs profile at DTRA-OM5.

Downhole Vs

High amplitude ambient noise was recorded at depth. Therefore, velocities below 36 m are low-confidence due to low signal-to-noise.

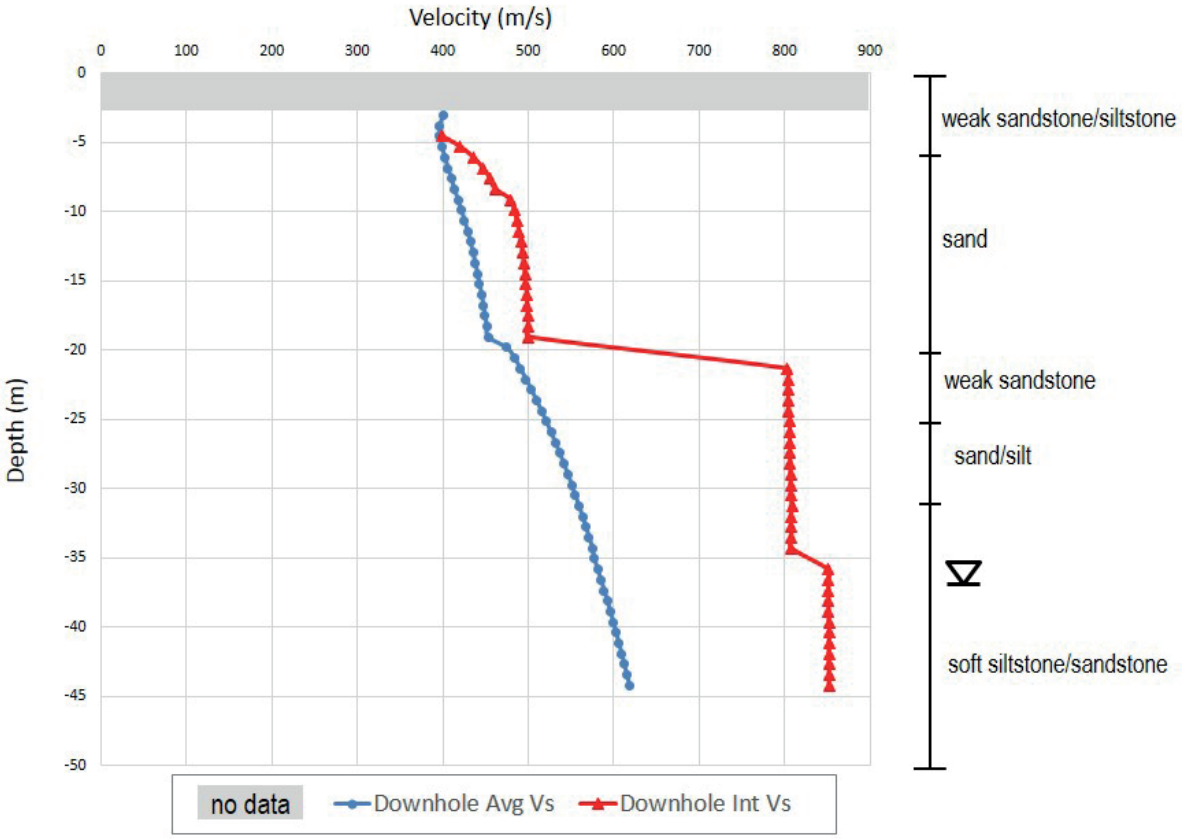

Figure 10: Downhole Vs profile at DTRA-OM5.

Downhole Vp

The waveform of direct P-wave recorded within receiver depths of 11.4 to 17.5 m is inconsistent with adjacent receiver depths (Figure 5a). This is suggestive of an anomaly outside the borehole casing. There are multiple possible sources of this phenomenon, and without additional information the exact cause is unclear. Arrival times, and thus velocity, on the nine traces within this interval have greater uncertainty. High amplitude ambient noise (i.e. traffic) was recorded at depth. Therefore, velocities below 36 m are low confidence due to low signal-to-noise.

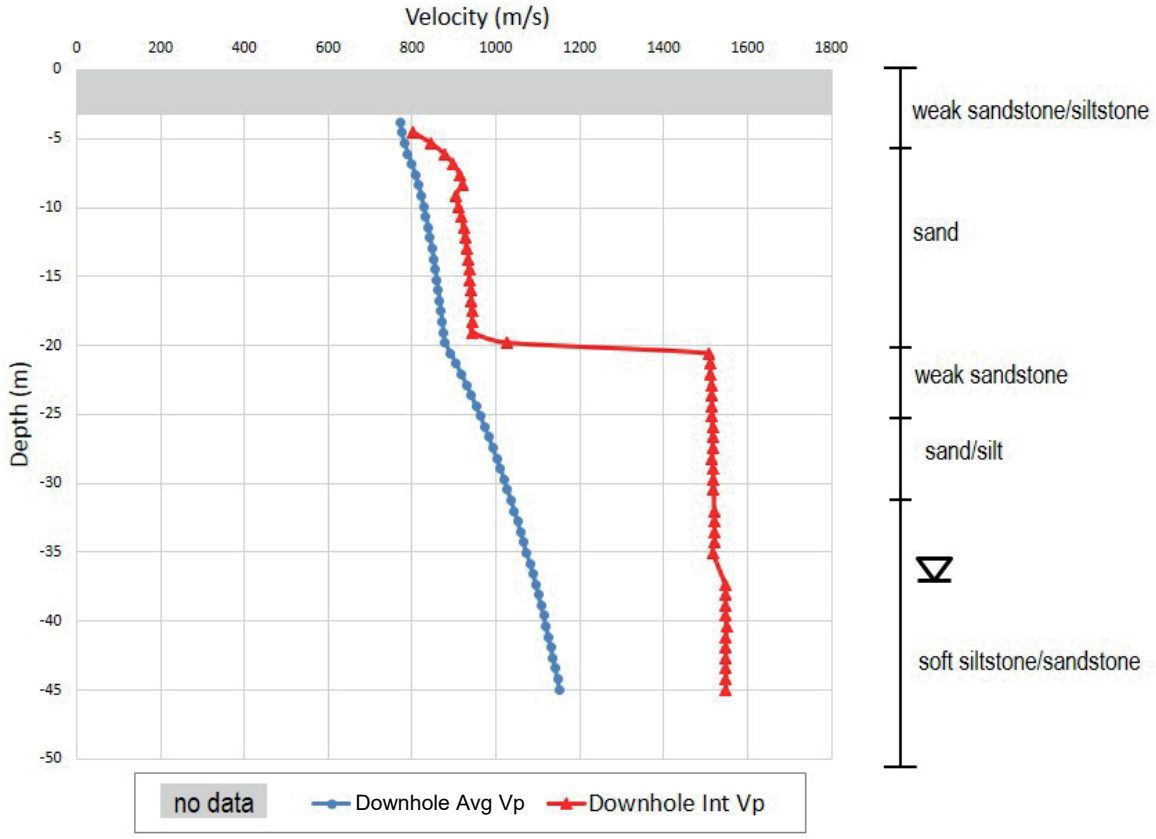

Figure 11: Downhole Vp profile at DTRA-OM5.

Vs Tomography

A smoothed version of the final MASW Vs profile was used as the initial model. Information from downhole seismic data improved discrimination of shear waves from mode-converted seismic energy. Shot records were re-picked to ensure accurate arrival times of the direct and refracted shear waves. In general, the resulting Vs tomography solution is a very good match to MASW. However, the downhole interval S-wave velocity is nearly 60% higher at 5 m depth. The significant difference in shallow velocity is realistic given the considerable distance (575 m) of the borehole from the surface seismic line.

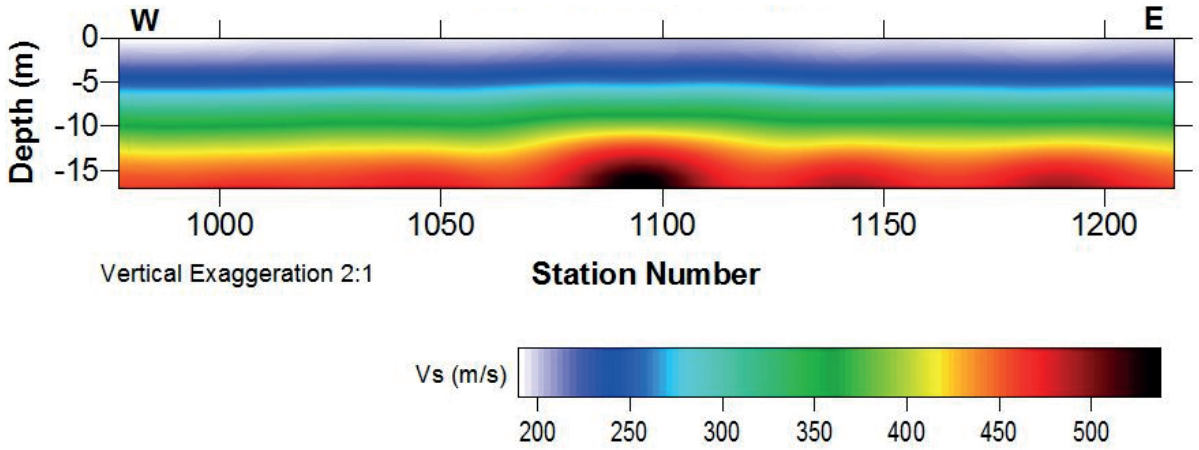

Figure 12: Vs tomography profile at DTRA-OM5.

Vp Tomography

A scaled, smoothed version of the final MASW Vs profile was used as the initial model. Picked first arrival times used for preliminary processing were reviewed and re-picked to increase accuracy of final processing. In general, the resulting Vp tomography solution follows the general trend of the Vs tomography solution, as expected for datasets acquired at a coincident location. The downhole interval P-wave velocity is nearly 45% higher at 5 m depth. The significant difference in shallow velocity is realistic given the considerable distance (575 m) of the borehole from the surface seismic line. In addition, refractions from a shallow high-velocity layer (~2500 m/s) were recorded on shot records at short offsets on the surface seismic line (Figure 13), indicating a velocity inversion that is not present at the borehole. This inversion is a violation of the assumption for refraction methods that velocity increases with depth. The high-velocity layer and hidden layer(s) beneath it cannot be accounted for, contributing to uncertainty in the tomography results.

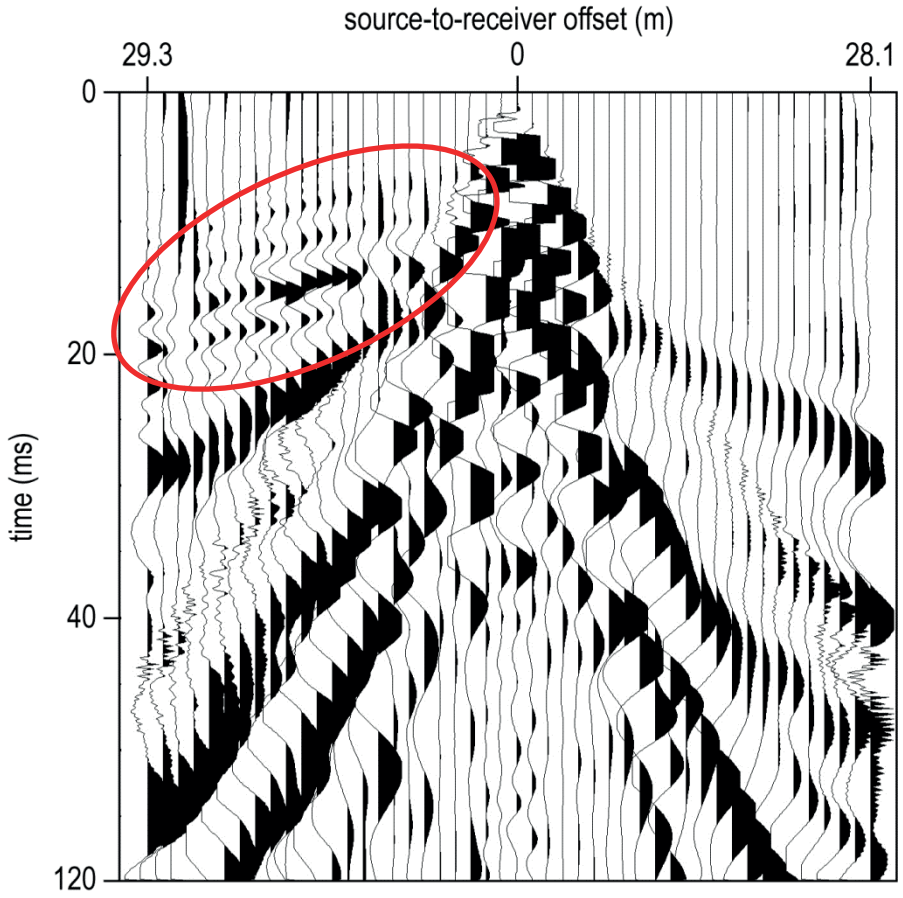

Figure 13: Shot record with a high-velocity refraction (circled in red).

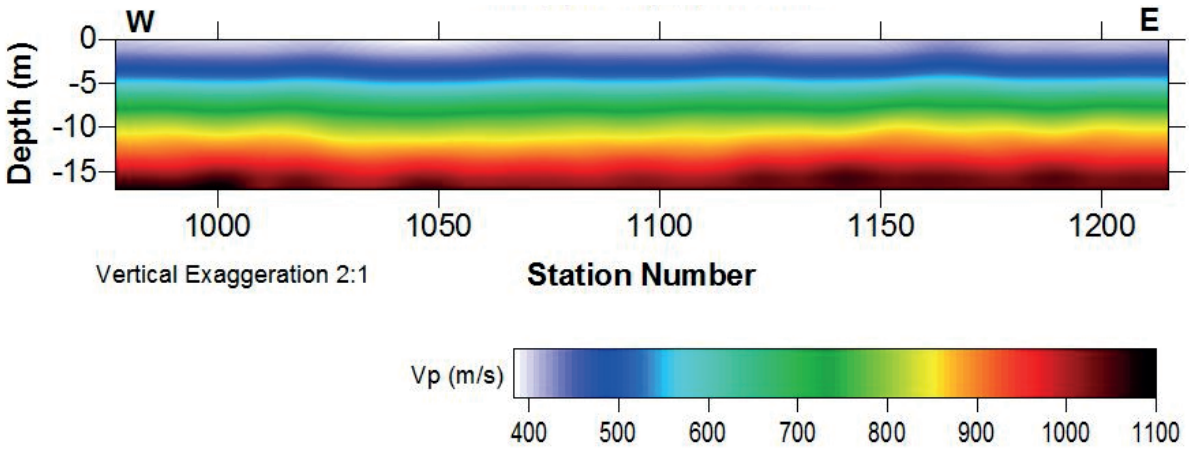

Figure 14: Vp tomography profile at DTRA-OM5.

Downhole Qs

Calculation of Q is highly sensitive to sources of noise (e.g., traffic) during acquisition.

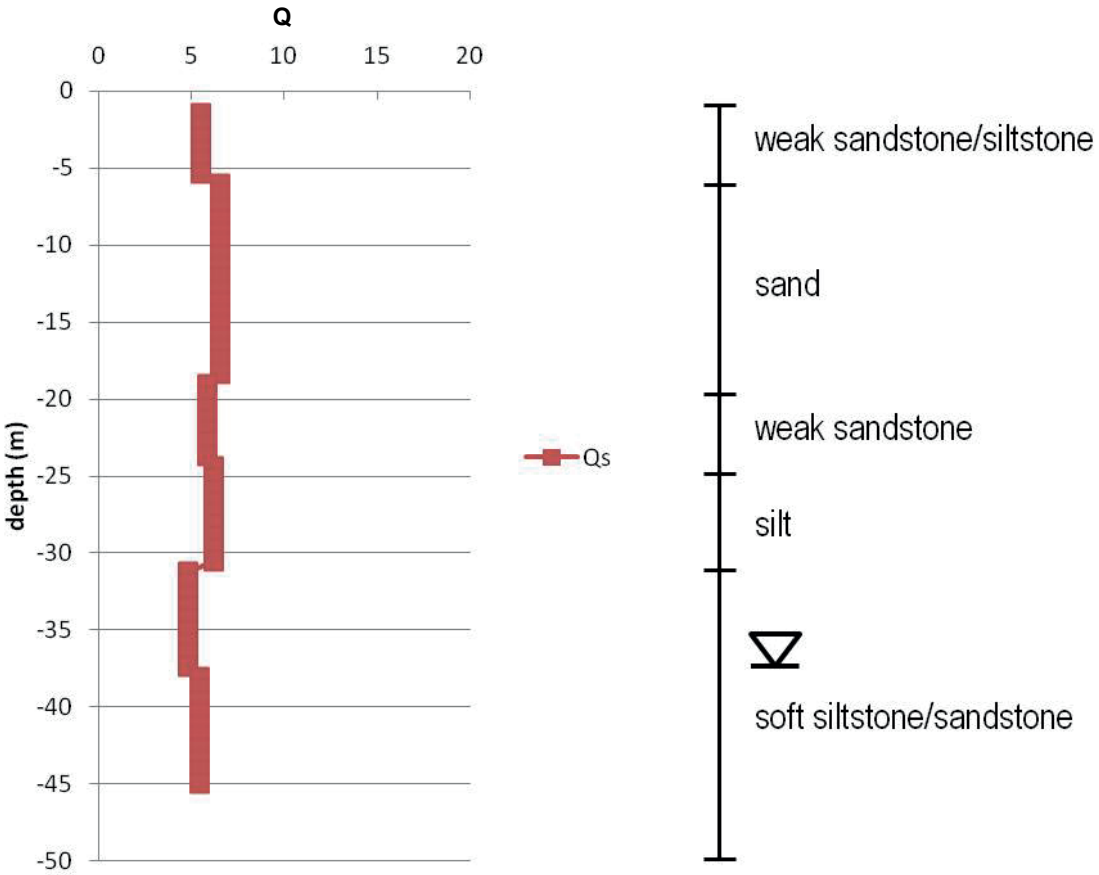

Figure 15: Downhole Qs profile at DTRA-OM5.

Downhole Qp

Calculation of Q is highly sensitive to sources of noise (e.g., traffic) during acquisition.

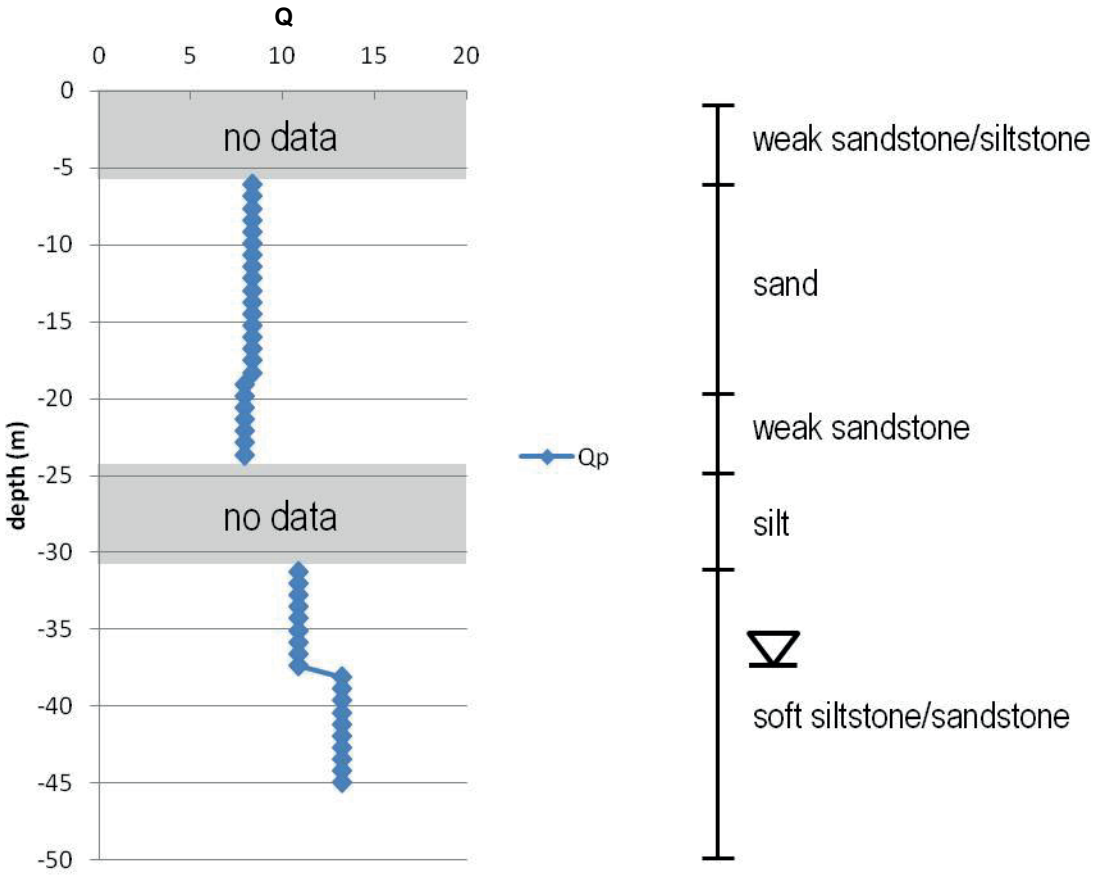

Figure 16: Downhole Qp profile at DTRA-OM5.

Surface Qs

Calculation of Q is highly sensitive to sources of noise (e.g., traffic) during acquisition. Due to lack of stability in the inversion, the upper 5 m is low confidence.

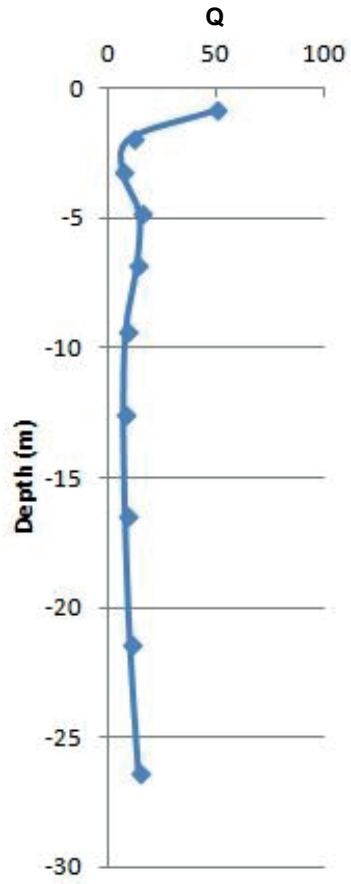

Figure 17: Surface Qs at DTRA-OM5.

Surface Qp

Calculation of Q is highly sensitive to sources of noise (e.g., traffic) during acquisition. Due to lack of stability in the inversion, the upper 5 m is low confidence.

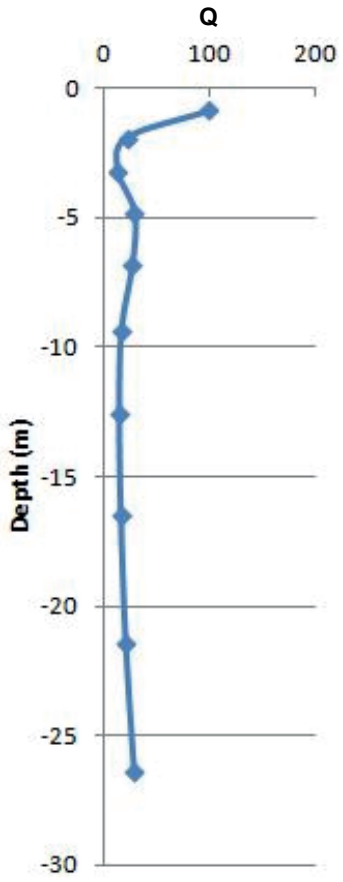

Figure 18: Surface Qp at DTRA-OM5.

Related Materials

Delivered materials include:

1. This report
2. PowerPoint presentation summarizing this report
3. Data files
4. Document explaining the data file format
5. Detailed list of deliverables

References

Di Siena, J.P., J.E. Gaiser, and D. Corrigan, 1984, Horizontal components and shear wave analysis of three component VSP data, in *Vertical Seismic Profiling, Part B: Advanced Concepts*, pp. 175-235, eds. M.N. Toksöz and R.R. Stewart, Geophysical Press, London.

Hasse, A.B. and R.R. Stewart, 2004, Attenuation estimates from VSP and log data: SEG expanded abstracts, 2497-2500.

Ivanov, J., R.D. Miller, J. Xia, J.B. Dunbar, and S. Peterie, 2010, Chapter 20: Refraction non-uniqueness studies at levee sites using the refraction-tomography and JARS methods: in Advances in Near-Surface Seismology and Ground-Penetrating Radar, SEG Geophysical Developments Series No. 15, R. D. Miller, J. D. Bradford, and K. Holliger, eds., Society of Exploration Geophysicists, 327-338.

Tonn, R., 1991, The determination of the seismic quality factor Q from VSP data: A comparison of different computational methods: *Geophysical Prospecting*, **39**, 1-27.

Xia, J., and R.D. Miller, 2010, Chapter 2: Estimation of near-surface shear-wave velocity and quality factor by inversion of high-frequency Rayleigh waves: in Advances in Near-Surface Seismology and Ground-Penetrating Radar, SEG Geophysical Developments Series No. 15, R. D. Miller, J. D. Bradford, and K. Holliger, eds., Society of Exploration Geophysicists, 17-36.

Xia, J., R.D. Miller, and C. B. Park, 1999, Estimation of near-surface velocity by inversion of Rayleigh waves: Geophysics, **64**, 691-700.